in hole size. These two processes, hole diffusion and lattice contraction, would occur simultaneously in a relaxing glass. This uniform lattice contraction could be the mechanism by which the overall free volume changes. Since diffusion of holes would be expected to occur slowly in the glassy state, this hole diffusion would be the rate-determining step. Well above the glass transition the hole diffusion and uniform contraction would occur at comparable rates.

Conclusion

We have presented a simple, nonlinear diffusion model that semiquantitatively reproduces the major phenomena observed during physical aging of glasses. We have also speculated on how a diffusion picture can be reconciled with sample-size independence of these annealing effects. Further work clearly needs to be done to elucidate the details of the diffusion mechanism. Nevertheless, we feel that the agreement with the phenomenological model strongly suggests that volume recovery behavior in glasses is due essentially to a diffusion process.

Acknowledgment. We acknowledge helpful discussions with R. R. Eaton, Sandia National Laboratories, who provided advice regarding the numerical solutions of the nonlinear diffusion equation. We also acknowledge several helpful discussions and suggestions by R. E. Robertson, Ford Motor Co.

References and Notes

(1) Kovacs, A. J. *Adv. Polym. Sci.* **1963**, *3*, 394.
(2) (a) Kovacs, A. J.; Aklonis, J. J.; Hutchinson, J. M.; Ramos, A. R. *J. Polym. Sci., Polym. Phys. Ed.* **1979**, *17*, 1097. (b) Gaskell, P. H., Ed. "The Structure of Non-Crystalline Materials"; Taylor and Francis: London, 1977; p 153.
(3) (a) Robertson, R. E. *J. Polym. Sci., Polym. Phys. Ed.* **1979**, *17*, 597. (b) Robertson, R. E. *Ann. N.Y. Acad. Sci.* **1981**, *371*, 21.
(4) Hirai, N.; Eyring, H. *J. Appl. Phys.* **1958**, *29*, 810.
(5) Haward, R. N., Ed. "The Physics of Glassy Polymers"; Wiley: New York, 1973; p 26.
(6) Simha, R.; Somcynsky, T. *Macromolecules* **1969**, *2*, 342.
(7) Curro, J. G.; Lagasse, R. R.; Simha, R. *J. Appl. Phys.* **1981**, *52*, 5892.
(8) Ferry, J. D. "Viscoelastic Properties of Polymers"; Wiley: New York, 1970.
(9) Cohen, M.; Turnbull, D. *J. Chem. Phys.* **1959**, *31*, 1164.
(10) Gartling, D. K. Coyote—A Finite Element Computer Program for Nonlinear Heat Conduction Problems, Sandia National Laboratories Report SAND 77-1332, 1978.
(11) Kovacs, A. J.; Stratton, R. A.; Ferry, J. D. *J. Phys. Chem.* **1963**, *67*, 152.
(12) (a) Simha, R.; Wilson, P. *Macromolecules* **1973**, *6*, 908. (b) McKinney, J. E.; Simha, R. *Macromolecules* **1974**, *7*, 894.
(13) Braun, G.; Kovacs, A. J. *Phys. Chem. Glasses* **1963**, *4*, 152.
(14) Montrose, C. J.; Litovitz, T. A. *J. Acoust. Soc. Am.* **1970**, *47*, 1250.
(15) Yeh, G. S. *Crit. Rev. Macromol. Sci.* **1972**, *1*, 173.
(16) Thomas, E. L.; Roche, E. J. *Polymer* **1979**, *20*, 1413.
(17) Hayler, L.; Goldstein, M. *J. Chem. Phys.* **1977**, *66*, 4736.
(18) Hoare, M. *Ann. N.Y. Acad. Sci.* **1976**, *279*, 186.
(19) Phillips, J. C. *Phys. Today* **1982**, *35*, 27.

Local Configuration of Poly(L-proline) in Dilute Solution

J. A. Darsey and Wayne L. Mattice*

Department of Chemistry, Louisiana State University, Baton Rouge, Louisiana 70803.
Received April 5, 1982

ABSTRACT: Representative poly(L-proline) chains containing peptide bonds in the trans configuration have been generated using a conformational energy surface that successfully reproduces the unperturbed dimensions in dilute solution. Representative chains have also been generated using selected portions of that surface in order to assess the influence of various features on the local conformation. Approach of the X component of the end-to-end vector to its asymptotic limit has been characterized for these same cases. In dilute solution, the overall configuration for chains containing as few as 70 prolyl residues is that of a random coil. Within the chain can be found a few short sequences that adopt a threefold left-handed helical structure reminiscent of that seen in the solid state. Threefold helices containing more than two turns are not seen in chains representative of the ensemble found in dilute solution. Helices do not extend further due to a continuous bending of the chain and, to a lesser extent, because of the presence of occasional sharp turns. The flexibility of the pyrrolidine ring plays a role in limiting the size of recognizable threefold helices.

Poly(L-proline) forms either of two ordered conformations in the solid state. Form I is a rather compact right-handed helix in which peptide bonds adopt the cis configuration,[1] and form II is a comparatively extended left-handed helix containing peptide bonds in the trans configuration.[2,3] In dilute solution there is a pronounced tendency for all peptide bonds to adopt the same configuration.[4-10] A reversible interconversion between the two forms can be produced by appropriate changes in solvent composition.[6,7,10] The configuration containing cis peptide bonds is favored in poor solvents. The tendency for aggregation in these solvents has prevented an extensive physical characterization of the solution conformational properties of form I. Good solvents support the chain configuration containing trans peptide bonds. Samples with weight-average molecular weights ranging from 4000 to 100 000 have been studied in five solvents that favor the form containing trans peptide bonds.[11] Behavior of the intrinsic viscosity over this molecular weight range demonstrates that the overall configuration is that of a random coil in a good solvent. The asymptotic limit for the characteristic ratio, $C = \langle r^2 \rangle_0 / n_p l_p^2$, is found to be 14 in water and 18–20 in three organic solvents at 25 °C.[11] Here $\langle r^2 \rangle_0$ denotes the mean square unperturbed end-to-end distance and n_p is the number of virtual bonds of length l_p. Virtual bonds extend from C^α of residue i to C^α of residue $i + 1$. They have length 380 pm.[12]

Measured characteristic ratios are rationalized by a conformational energy surface that incorporates consequences of flexibility in the pyrrolidine ring.[13] The major feature in the conformational energy surface is an area of low energy that includes the conformation adopted by a prolyl residue in the solid state. This low-energy region has an extension of about 80° for the C^α–C′ dihedral angle, ψ, and an extension about half as large for the C^α–N dihedral angle, ϕ. The limiting characteristic ratio for

0024-9297/82/2215-1626$01.25/0

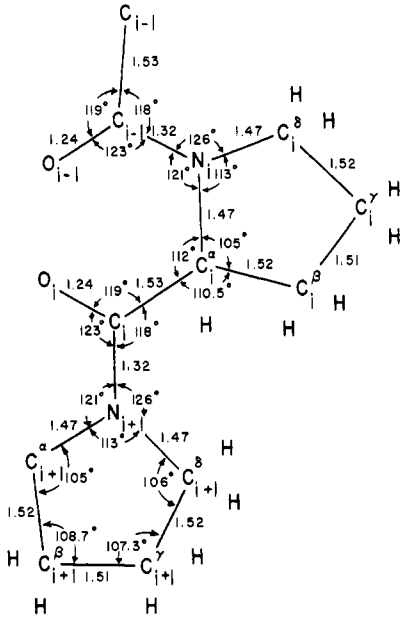

Figure 1. Bond lengths and angles between bonds for poly(L-proline). This figure is taken from ref 13.

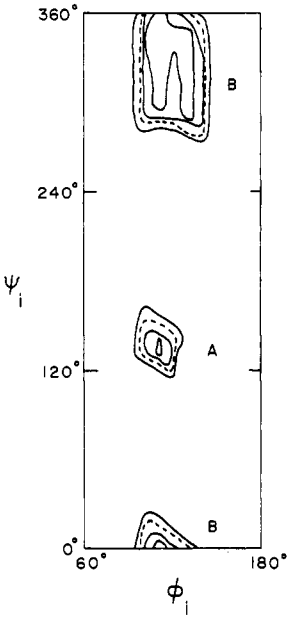

Figure 2. Conformational energy surface for a prolyl residue in poly(L-proline). This conformational energy surface is the one labeled $\gamma 1$ by Mattice et al.[13] Contours are drawn at energies 1, 2, 5, and 10 kcal/mol above the minimum energy.

poly(L-proline) would have been near 30 if this region were the only accessible feature on the conformational energy surface. However, there is a second, more restricted, and somewhat higher, energy minimum displaced from the major minimum by about 180°. This second feature of the conformational energy surface causes the computed characteristic ratio to move into the range defined by experiment. These results clearly demonstrate that the unperturbed dimensions of poly(L-proline) in solution demand occasional occupancy of a second region of low energy on the conformational energy surface. The necessary reduction in unperturbed dimensions might also be supplied by the presence of a few randomly located cis placements about the peptide bond,[14] particularly in aqueous solution.[15] However, random cis placements are not observed in organic solvents such as trifluoroethanol,[16] in which the characteristic ratio is 18–20.[11]

One objective here is examination of the manner in which features of the conformational energy surface described by Mattice et al.[13] affect the local structure of representative poly(L-proline) chains. Special attention will be given to the extent to which the local structure of the chain in solution retains a threefold helical conformation reminiscent of that adopted in the solid state. A second objective is characterization of the behavior of the average projection of a unit vector along the last virtual bond onto a unit vector along the first virtual bond.

Calculations

Bond lengths and angles between bonds are depicted in Figure 1, and the conformational energy surface is depicted in Figure 2. This conformational energy surface differs from the $\gamma 1$ map described by Mattice et al.[13] only in adoption of the convention in which dihedral angles become zero in the fully extended polypeptide chain. Representative chains were generated using a pseudo random number generator and the assumption that prolyl residues behave independently. The probability $p_{\phi,\psi}$ that a prolyl residue would occupy a specified conformation was

$$p_{\phi,\psi} = \exp(-E_{\phi,\psi}/RT)/[\sum_{\phi}\sum_{\psi}\exp(-E_{\phi,\psi}/RT)] \quad (1)$$

Several representative chains were generated for each conformational energy surface and found to have similar characteristics. For example, squared end-to-end distances for representative chains differed only slightly from the $\langle r^2\rangle_0$ evaluated for the conformational energy surface in use. Representative chains selected for description here are those in which, from the viewpoint established by the plotting routine, the features of interest are most easily seen.

The average transformation matrix for a prolyl residue was calculated as

$$\langle \mathbf{T} \rangle = \mathbf{T}_\omega \sum_{\phi}\sum_{\psi} p_{\phi,\psi}\mathbf{T}_\phi\mathbf{T}_\psi \quad (2)$$

where $\mathbf{T}_\omega$, $\mathbf{T}_\phi$, and $\mathbf{T}_\psi$ denote transformation matrices for the peptide, C^α–N, and C^α–C′ bonds, respectively.[12] A 10° increment was used in evaluation of all summations. Conformations where the energy exceeded the minimum energy by more than 10 kcal/mol were excluded. All of the remaining conformational energy surface was included unless stated to the contrary. The average projection of a unit vector along the final virtual bond onto a unit vector along the first virtual bond is

$$\langle A_{xx} \rangle = \text{row } (1, 0, 0)\langle \mathbf{T} \rangle^{n_p-1} \text{ col } (1, 0, 0) \quad (3)$$

Results and Discussion

Figure 3 depicts a poly(L-proline) chain in which all residues adopt the conformation with $\phi, \psi = 103.7°, 325.1°$. The rodlike nature of this configuration is readily apparent. The chain depicted shows a very slight deviation from a helix with precisely three prolyl residues per turn. This deviation becomes apparent if every third pyrrolidine ring is traced from one end of the chain to the other. The slight deviation from a helix with precisely three prolyl residues per turn presumably arises from slight differences between bond angles used in our chain and those assumed by Sasisekharan[3] in his characterization of form II in the solid state.

Long chains cease to have the overall architecture of a rod when each prolyl residue has access to the conformational energy surface depicted in Figure 2. This conclusion is supported by the representative chain of 60 prolyl residues depicted in Figure 4. The value of $r^2/n_p l_p^2$ for the representative chain is 11, which is close to the asymptotic limit of 12.4 (Table I) obtained for C when averaging takes

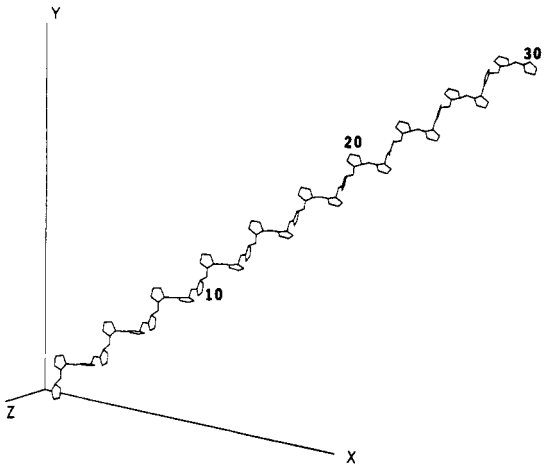

Figure 3. Poly(L-proline) chain of 30 residues in which all ϕ are 103.7° and all ψ are 325.1°. This figure depicts all C–C and C–N bonds.

Table I
Characteristics of Poly(L-proline) Chains Sampling Different Conformational Energy Surfaces

surface	C	$1/\tau$	oscillations[a]	local maxima[b]	turns[c]
all	12.4	8	40	0	2
region B	29	29	150	3	2
ϕ = 110°	9.5	5	30	0	2
ϕ = 110°, region B	42	20	160	3	3

[a] Approximate n_p at which oscillations in $\langle A_{xx} \rangle$ are no longer detectable on the scale used in Figures 5, 7, 9, and 11. [b] Local maxima at $n_p > 1$ when $\langle A_{xx} \rangle$ is examined for chains with $3i + 1$ virtual bonds. [c] Largest number of turns in a single threefold helix in the representative chain depicted in Figures 4, 6, 8, and 10.

place over all chains in the ensemble. While this representative chain clearly has the overall shape of a random coil, short segments can be found that have a conformation reminiscent of the threefold helix found in the solid state. These short segments are more easily identified if pyrrolidine rings are included in the depiction of the representative chain. Identification of threefold helical segments containing at least two turns can be achieved by a search for cases where pyrrolidine rings i, $i + 3$, and $i + 6$ lie along a straight line and have the same orientation with respect to this line. The best example in the representative chain depicted in Figure 4b is provided by prolyl residues 8, 11, and 14. These prolyl residues are identified by asterisks. No threefold helical segments can be found that contain as many as three turns.

The helical segments including prolyl residues 8, 11, and 14 becomes continuously disordered as one proceeds from residue 8 to residue 1. The chain is seen to undergo a sharp turn as one proceeds in the other direction from residue 14 to residue 20. The sharp turn arises because prolyl residue 18 in this chain adopts a conformation found in the low-energy region denoted by A in Figure 2. Residues adopting a configuration in this region are denoted by A in the depiction of representative chains. A second sharp turn is apparent at residue 45, which also adopts a configuration in the smaller region of low conformational energy. The continuous bending and the sharp turns contribute to the overall architecture being that of a random coil rather than a rod. They also impose an upper limit on the number of residues in a sequence whose conformation can accurately be described as a threefold

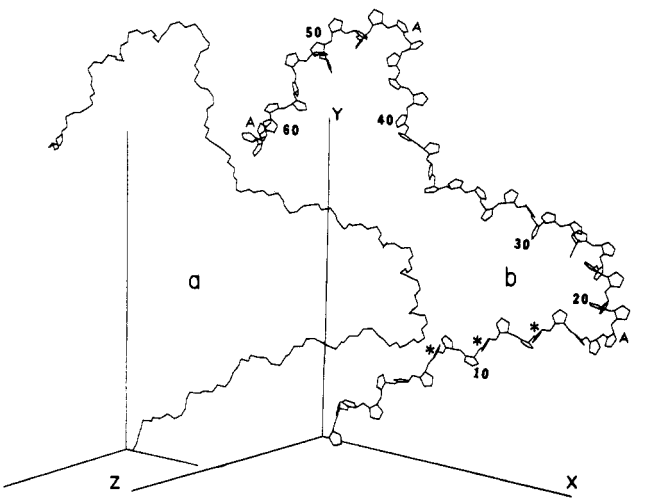

Figure 4. Representative poly(L-proline) chain of 60 residues in which the conformational energy surface accessible to each residue is that depicted in Figure 2. The chain in (b) depicts all C–C and C–N bonds, while that in (a) shows only those C–C and C–N bonds in the main chain. Coordinates of the last C^α atom are X = −7.58 nm, Y = 1.7 nm, Z = −5.78 nm, and $r^2/n_p l_p^2$ is 11.

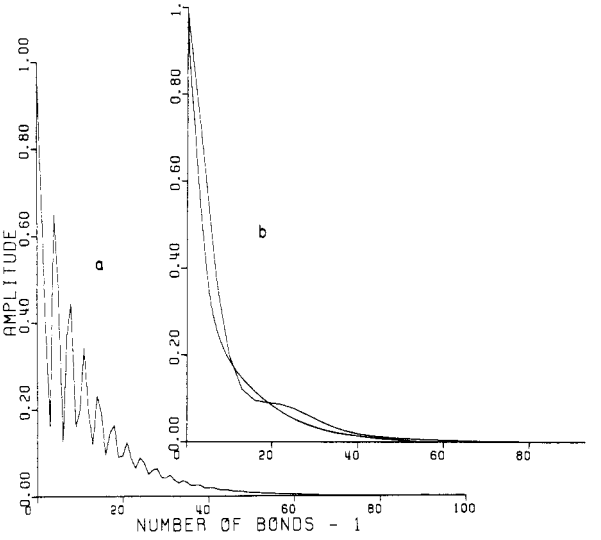

Figure 5. Average projection of a unit vector along the last virtual bond onto a unit vector along the first virtual bond. Prolyl residues sample the conformational energy surface depicted in Figure 2. The plot in (a) shows every virtual bond, while that in (b) depicts virtual bonds $3i + 1$. The smooth curve in (b) is the exponential curve $\exp[-\tau(n_p - 1)]$ described in the text.

helix. Relative importance of the continuous bending and sharp turns will be brought out by other representative chains to be discussed below.

Figure 5 depicts the average projection of a unit vector along the last virtual bond onto a unit vector lying along the first virtual bond. The chain depicted in Figure 4 is representative of the ensemble treated in Figure 5. Figure 5a shows an exponential decay on which is superimposed a threefold oscillation at small n_p. Oscillations remain detectable up to n_p slightly above 40 on the scale used in this figure. Hence they extend over a number of residues which is about $^2/_3$ as large as the degree of polymerization of the representative chain depicted in Figure 4. In Figure 5b data are restricted to those chains in which n_p is $3i + 1$. The curve is nearly that described by a critically damped harmonic oscillator. It can be approximated as $\exp[-\tau(n_p - 1)]$, with $\tau = 0.128$, as shown in Figure 5b. If $1/\tau$ is treated as a correlation length, its value of 7.8 is comparable to the number of residues that can be found

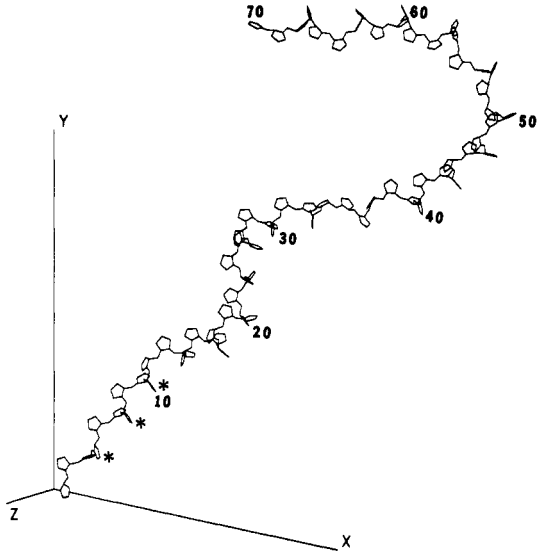

Figure 6. Representative poly(L-proline) chain of 70 residues. Prolyl residues are restricted to the low-energy region labeled B in Figure 2. Coordinates of the last C^{α} atom are X = 8.73 nm, Y = 10.50 nm, Z = 5.00 nm, and $r^2/n_p l_p^2$ = 21.

in a threefold helical segment in the representative chain depicted in Figure 4. Results to be presented below demonstrate that the agreement between $1/\tau$ and the length of a helical segment is fortuitous.

Exclusion of the Second Minimum. Figure 6 depicts a representative poly(L-proline) chain in which the small low-energy region labeled A in Figure 2 is forbidden. For this representative chain, $r^2/n_p l_p^2$ is 21, which is slightly smaller than the asymptotic limit for C (Table I) for this ensemble. This representative chain shares several features with the one depicted in Figure 4. Both chains contain recognizable segments of threefold helix covering a span as long as residues i, $i + 3$, and $i + 6$. Residues 4, 7, and 10 in Figure 6 show this feature. Significantly longer segments with a precise threefold nature are absent. Flexibility of the chains in both Figures 4 and 6 is sufficient to produce the overall shape of a random coil. The major difference in the two representative chains lies in the absence of sharp turns in the one depicted in Figure 6. The sharp turns seen in Figure 4 arise from occasional residues that occupy the small energy minimum, and consequently such turns must be absent in the chain depicted in Figure 6. Sharp turns are of sufficiently rare occurrence in Figure 4 that their deletion from the chain does not significantly alter the maximum length of threefold helical segments. Therefore the limitation on the length of threefold helical segments arises from the flexibility associated with the major low-energy region in the conformational energy surface. The occasional sharp turns seen in Figure 4 do produce a much more compact overall configuration, as expected. The asymptotic limit for C falls by more than a factor of 2 when the minor minimum is included in the conformational energy surface (Table I).

Figure 7 depicts $\langle A_{xx} \rangle$ when each prolyl residue is restricted to the major low-energy region in the conformational energy surface. Oscillations are still detectable in Figure 7a when the number of virtual bonds exceeds 100. Inclusion of the minor low-energy region would have caused $\langle A_{xx} \rangle$ to decay to zero before n_p becomes as large as 100 (Figure 5a). Attention is restricted to chains containing $3i + 1$ virtual bonds in Figures 5b and 7b. Exclusion of the minor minimum from the conformational energy surface is seen to change the behavior from that of an oscillator which is very nearly critically damped to

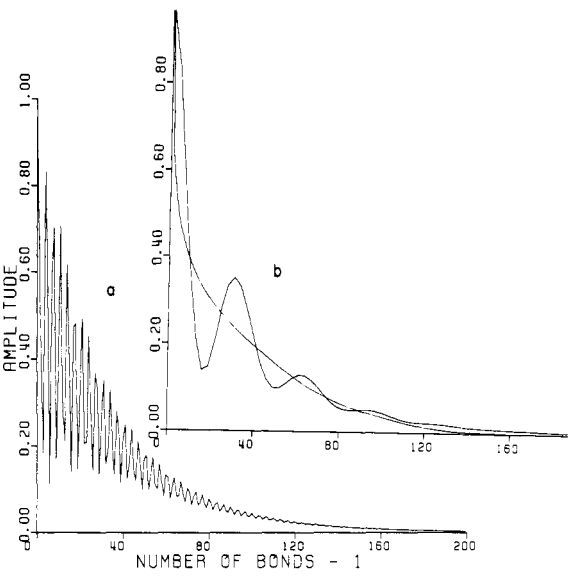

Figure 7. Average projection of a unit vector along the last virtual bond onto a unit vector along the first virtual bond. Prolyl residues are restricted to the major low-energy region of the conformational energy surface depicted in Figure 2. The curve in (a) shows every virtual bond, while that in (b) depicts virtual bonds $3i + 1$.

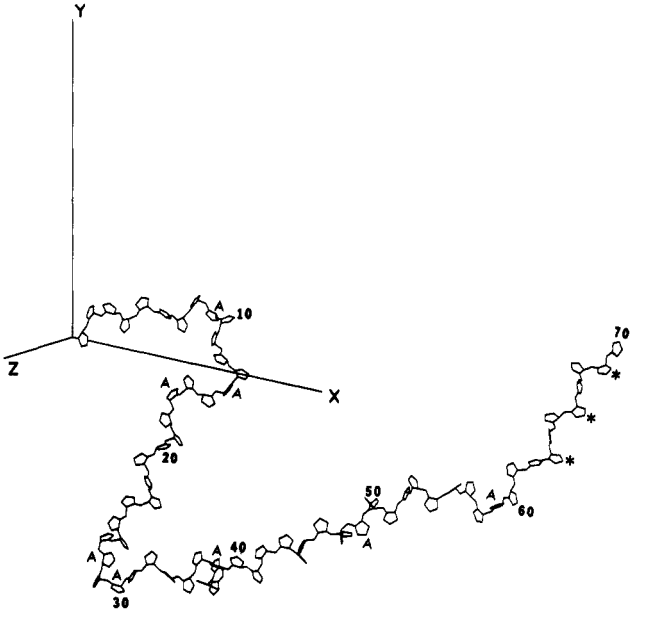

Figure 8. Representative poly(L-proline) chain of 70 residues in which each residue has ϕ = 110°. Coordinates of the last C^{α} atom are X = 6.42 nm, Y = −0.50 nm, Z = −6.55 nm, and $r^2/n_p l_p^2$ = 8.5.

that of an underdamped harmonic oscillator. The best exponential fit to the decay of the midpoint about which oscillation occurs in Figure 7b yields τ = 0.035. The reciprocal is nearly 30, which is clearly much larger than the length of any recognizable helical segment in the representative chain depicted in Figure 6. The fourfold decrease in τ from Figure 7b to Figure 5b reflects the large effect occupancy of a state much different from that of the threefold helix can have on correlations between the first and last virtual bond.

Restriction of ϕ to 110°. Figure 8 depicts a representative chain in which all prolyl residues have ϕ restricted to 110°. The pyrrolidine ring is therefore considered to be rigid. Both low-energy regions in Figure 2 contribute to the residue configuration partition function. The representative chain has $r^2/n_p l_p^2$ = 8.5, which stands

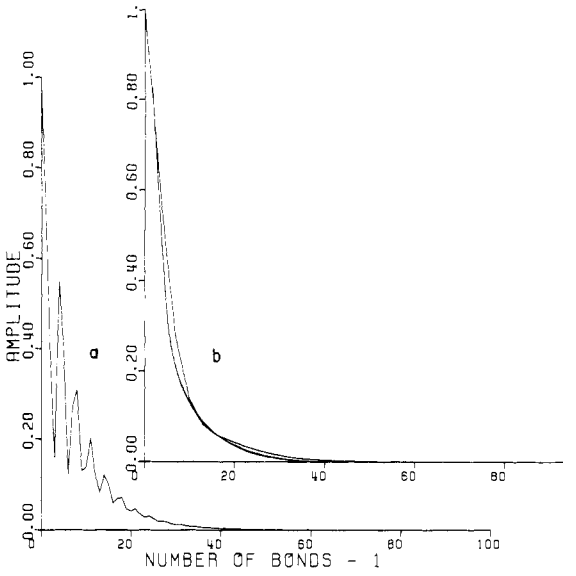

Figure 9. Average projection of a unit vector along the last virtual bond onto a unit vector along the first virtual bond. Each prolyl residue has $\phi = 110°$. The curve in (a) shows every virtual bond, while that in (b) depicts virtual bonds $3i + 1$.

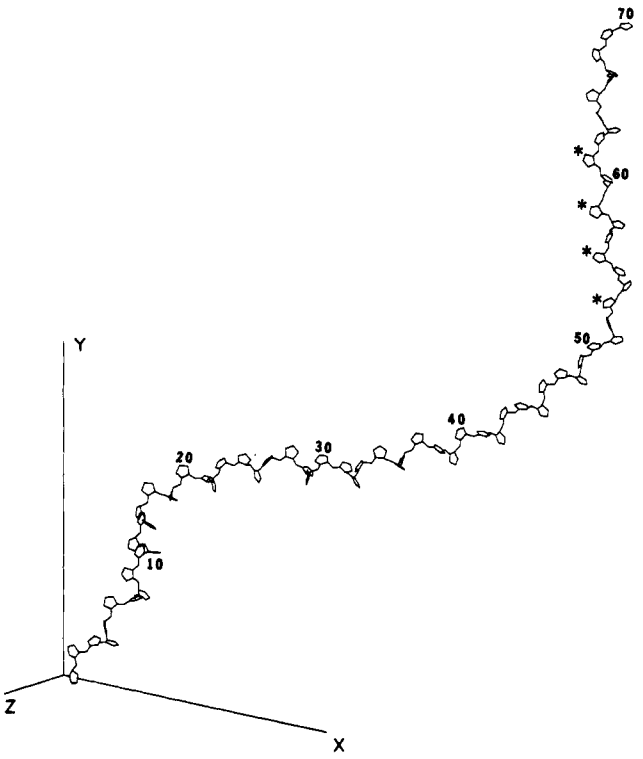

Figure 10. Representative poly(L-proline) chain of 70 residues in which each residue has $\phi = 110°$ and ψ is restricted to $330 \pm 30°$. Coordinates of the last C^α atom are $X = 11.86$ nm, $Y = 9.90$ nm, $Z = -10.66$ nm, and $r^2/n_p l_p^2 = 35$.

in excellent agreement with $C = 9.5$ (Table I). Sharp turns are again present. They are more frequent than was the case in Figure 4 because ϕ has been restricted to the value that yields the minimum energy in region A of the conformational energy surface in Figure 2. Behavior of $\langle A_{xx} \rangle$, depicted in Figure 9, is reminiscent of that seen (Figure 5) when the entire conformational energy surface was accessible. The best value for τ is about 0.21.

Simultaneous Restriction to the Major Low-Energy Region and $\phi = 110°$. Figure 10 depicts a representative chain in which all prolyl residues have $\phi = 110°$ and ψ is restricted to the major low-energy region on the conformational energy surface of Figure 2. The representative chain depicted has $r^2/n_p l_p^2 = 35$, while the average over all chains in the ensemble yields $C = 42$. Sharp turns are absent, and recognizable stretches of threefold helix can now be found that extend for as many as three turns (asterisks in Figure 10). The behavior of $\langle A_{xx} \rangle$ (Figure 11) is reminiscent of that seen when all prolyl residues were restricted to the major region of low conformational energy (Figure 7).

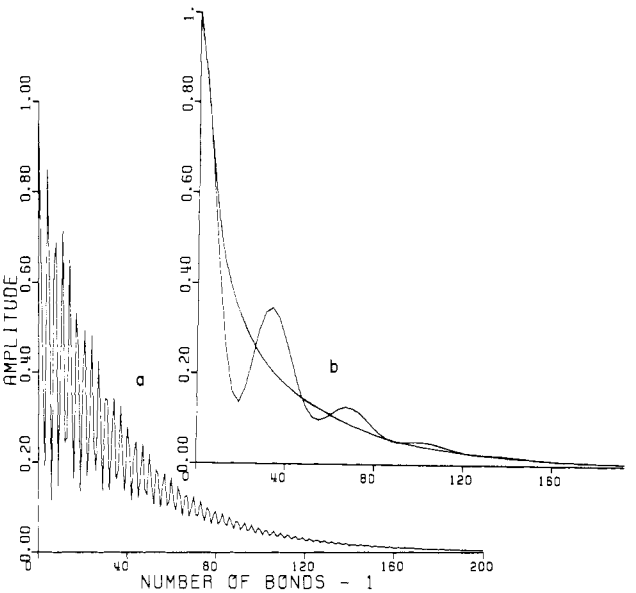

Figure 11. Average projection of a unit vector along the last virtual bond onto a unit vector along the first virtual bond. Prolyl residues have $\phi = 110°$, $\psi = 330 \pm 30°$. The curve in (a) shows every virtual bond, while that in (b) depicts virtual bonds $3i + 1$.

Correlates with Maximum Threefold Helix Length. Table I summarizes limiting characteristic ratios, features seen in the behavior of $\langle A_{xx} \rangle$, and a somewhat subjective measure of the longest threefold helix seen in representative chains. Many of these features (characteristic ratio, $1/\tau$, value of n_p at which oscillations in $\langle A_{xx} \rangle$ cease, and number of local maxima in $\langle A_{xx} \rangle$ for chains with $3i + 1$ virtual bonds) are seen to be most sensitive to the inclusion or exclusion of the minor region of low conformational energy. Each of these four parameters assumes larger values when the minor region of low energy is excluded. These properties are reduced by the occasional sharp turns produced when a prolyl residue occupies a configuration in the minor region of low conformational energy.

The maximum number of turns in a recognizable threefold helix in the representative chains is a more subjective quantity than the others listed in Table I. In recognition of its subjective character, entries in Table I for this term might be treated as being essentially indistinguishable. That in itself would be an important statement, for it would assert an insensitivity of the maximum helix length in poly(L-proline) in solution to changes in the conformational energy surface which are responsible for marked alteration in other configuration-dependent properties.

If the differences between two and three turns in the last column in Table I are deemed significant, they point to a role of the accessible range for ϕ in determination of the maximum helix length. The threefold helix must be composed of prolyl residues that occupy the major low-energy region in the conformational energy surface. The minor minimum contributes only about 6% of the residue partition function. Occupancy of the minor minimum will not

place the upper bound on the length of a threefold helix. The average number of prolyl residues separating those occupying the minor region of low conformational energy is about 17, which is significantly larger than the 7–8 residues found in the longest threefold helices in the representative chain depicted in Figure 4. Therefore the origin of the upper limit must lie in the major region of low conformational energy.

The shape attributed to the major region of low conformational energy depends on the choice of the contour line used to define that shape. The shape is nearly rectangular if the contour used is that at 5 or 10 kcal/mol. For present purposes the boundary of this region is better described by the 1 kcal/mol contour line. Most prolyl residues will adopt conformations within this contour, and the local configuration required for propagation of a precisely threefold helix is to be found here. The upper limit to the number of turns in a recognizable threefold helix is provided by the slight flexibility about ψ when ϕ is held constant at 110° and the minor region of low conformational energy is ignored. The representative chain depicted in Figure 10 shows this upper limit to be about three turns. A significant fraction of the prolyl residues adopt ϕ near 130° when the constraint on ϕ is relaxed. There is then an additional disordering influence on the chain and consequent reduction in the maximum length of recognizable threefold helix from three turns to two. Since a change in ϕ requires an alteration in geometry of the pyrrolidine ring system, the flexibility of this ring plays a role in establishing the upper limit for the length of recognizable threefold helices for poly(L-proline) in solution. The pyrrolidine ring of poly(γ-hydroxy-L-proline) is less flexible than that in poly(L-proline).[17-20] Consequently, the maximum length of recognizable threefold helices should be somewhat larger in poly(γ-hydroxy-L-proline) than that found here for poly(L-proline).

Acknowledgment is made to the donors of the Petroleum Research Fund, administered by the American Chemical Society, for partial support of this research.

References and Notes

(1) Traub, W.; Shmueli, U. *Nature (London)* **1963**, *198*, 1165.
(2) Cowan, P. M.; McGavin, S. *Nature (London)* **1955**, *176*, 501.
(3) Sasisekharan, V. *Acta Crystallogr.* **1959**, *12*, 897.
(4) Harrington, W. F.; Sela, M. *Biochim. Biophys. Acta* **1958**, *27*, 24.
(5) Steinberg, I. Z.; Harrington, W. F.; Berger, A.; Sela, M.; Katchalski, E. *J. Am. Chem. Soc.* **1960**, *82*, 5263.
(6) Gornick, F.; Mandelkern, L.; Diorio, A. F.; Roberts, D. E. *J. Am. Chem. Soc.* **1964**, *86*, 2549.
(7) Engel, J. *Biopolymers* **1966**, *4*, 945.
(8) Swenson, C. A.; Formanek, R. *J. Phys. Chem.* **1967**, *71*, 4073.
(9) Isemura, T.; Okabayashi, H.; Sakakibara, S. *Biopolymers* **1968**, *6*, 307.
(10) Ganser, V.; Engel, J.; Winklmair, D.; Krause, G. *Biopolymers* **1970**, *9*, 329.
(11) Mattice, W. L.; Mandelkern, L. *J. Am. Chem. Soc.* **1971**, *93*, 1769.
(12) Brant, D. A.; Flory, P. J. *J. Am. Chem. Soc.* **1965**, *87*, 2791.
(13) Mattice, W. L.; Nishikawa, K.; Ooi, T. *Macromolecules* **1973**, *6*, 443.
(14) Tanaka, S.; Scheraga, H. A. *Macromolecules* **1975**, *8*, 623.
(15) Wu, C. C.; Komoroski, R. A.; Mandelkern, L. *Macromolecules* **1975**, *8*, 635.
(16) Clark, D. S.; Dechter, J. J.; Mandelkern, L. *Macromolecules* **1979**, *12*, 626.
(17) Torchia, D. A. *Macromolecules* **1971**, *4*, 440.
(18) Torchia, D. A. *Macromolecules* **1972**, *5*, 566.
(19) Torchia, D. A.; Lyerla, J. R., Jr. *Biopolymers* **1974**, *13*, 97.
(20) Ooi, T.; Clark, D. S.; Mattice, W. L. *Macromolecules* **1974**, *7*, 337.

Notes

Orthorhombic vs. Monoclinic Structures for the α and γ Phases of Poly(vinylidene fluoride): An Analysis

STEVEN WEINHOLD, MICHAEL A. BACHMANN,† MORTON H. LITT, and JEROME B. LANDO*

Department of Macromolecular Science, Case Western Reserve University, Cleveland, Ohio 44106.
Received April 20, 1982

Recently, we investigated the crystal structures of the α, γ, and δ crystal forms of poly(vinylidene fluoride).[1-4] This effort was precipitated by the realization that the crystal structure of the γ phase originally proposed by Hasegawa et al.[5] was inconsistent with the X-ray fiber (and powder) diffraction pattern of that material.[1] Our structure analysis of the γ phase[2] appeared simultaneously with a short communication from Takashashi and Tadokoro[6] describing the results of a new investigation into the structure of the γ phase. The results of the two investigations are summarized in Table I. While the two structures are basically very similar, a few significant differences do exist. The most significant discrepancy is that the structure proposed by us is orthorhombic, while that proposed by Takahashi and Tadokoro belongs to the monoclinic crystal system. The higher symmetry of our proposed structure is due to the statistical parallel–antiparallel chain packing we believe to be present; if this packing were replaced by exclusively parallel chains, as is the case in the structure of Takahashi and Tadokoro, the symmetry of the resulting structure would be monoclinic even though the cell remained orthogonal.

After determining the structure of the γ phase, we investigated that of the δ phase and found that statistical parallel–antiparallel chain packing appeared to be present in that material as well.[3] These results suggested that this sort of statistical packing might also be present in the α phase of PVF_2, and so we reinvestigated that structure.

Two investigations into the structure of the α phase had already been performed: one by Doll and Lando[7] and, shortly thereafter, one by Hasegawa et al.[5] In our reinvestigation we employed the observed intensity data set of Hasegawa et al.[5] because it was the more complete of the two available. Our investigation confirmed the following points: the chain conformation proposed by Hasegawa et al. was preferable to the slightly different conformation originally proposed by Doll and Lando. The orientation of the chains about their axis is such that the component of the net chain dipole moment normal to the chain axis is directed in exactly the [100] direction, in agreement with the results of Hasegawa et al. and con-

†Current address: Owens Corning Fiberglas Technical Center, Granville, OH 43023.

0024-9297/82/2215-1631$01.25/0